



ELSEVIER

Physica E 13 (2002) 109–113

PHYSICA E

www.elsevier.com/locate/physce

# Electron dynamics of a single quantum dot probed with wideband millimeter-wave spectroscopy

Hua Qin<sup>a</sup>, Robert H. Blick<sup>a,\*</sup>, Daniel W. van der Weide<sup>b</sup>, Karl Eberl<sup>c</sup>

<sup>a</sup>Center for NanoScience and Sektion Physik, Ludwig-Maximilians-Universität, Geschwister-Scholl-Platz 1, 80539 München, Germany

<sup>b</sup>Department of Electrical and Computer Engineering, University of Wisconsin, 1415 Engineering Dr, Madison, WI 53706, USA

<sup>c</sup>Max-Planck-Institut für Festkörperforschung, Heisenbergstr. 1, 70569 Stuttgart, Germany

## Abstract

We perform microwave spectroscopy on a single quantum dot using a compact pulsed spectrometer. Although DC transport shows strong elastic cotunneling in the Coulomb blockade regime and inelastic tunneling in the single-electron tunneling (SET) regime, these effects are suppressed under picosecond impulses whose energies are commensurate with those of the dot. Instead, under non-zero bias we find excited-state resonances in the induced complex photoconductance as well as strong deviations of the dot capacitance compared to equilibrium values, a signature of the effective relaxation times of SET. © 2002 Elsevier Science B.V. All rights reserved.

PACS: 07.57.Hm; 73.23.Hk; 73.21.La

Keywords: Millimeter wave; Coulomb blockade and SET; Quantum dots

Structured quantum dots are few-electron systems useful not only as models of atoms and molecules but also in quantum computation [1]. The dots—droplets of electrons—are usually electrostatically confined by nanometer sized gates and coupled to leads, enabling transport spectroscopy at DC [2]. Coherent superpositions of covalent molecular states of tunnel-coupled quantum dots have been realized by applying continuous microwaves [3,4]. Pulsed microwaves are desired to control the superpositions of molecular states [5], i.e. sampling of a quantum bit (qubit). On the other hand, pulsed microwaves are expected to switch qubits for simple quantum computing operations. Characterizations of dynamic responses of electrons in

quantum dots to the microwave pulses are thus essential. Time-resolved measurements of Cooper pair tunneling in coupled Josephson junctions by Nakamura et al. [6] have spurred interest in using temporal information to study the electron dynamics of dots. Recently, electron dynamics have been investigated in single electrostatically defined quantum dots using different techniques [7].

Here we present photoconductance measurements on a single laterally gated quantum dot in the few electron limit using a wideband, i.e. pulsed, millimeter-wave spectrometer. The quantum dot is first characterized by conventional transport spectroscopy, which is then compared to the photoconductance spectra. By downconverting the millimeter-wave signal coherently via a beat note between two microwave sources, the amplitude and phase of the conductance can be determined. The spectrometer

\* Corresponding author. Tel.: +49-89-2180-3733; fax: +49-89-2180-3182.

E-mail address: robert@nanomachines.com (R.H. Blick).

allows us to observe excited states of the quantum dot and trace these states even at non-zero bias. It enables us to reveal the time-dependent variation of the quantum dot's capacitance. Finally, since we detect harmonics with a lock-in amplifier, we can perform broadband spectroscopy on the dot system without changing the heat load in contrast to conventional tuned sources, such as Gunn diodes.

The spectrometer itself consists of two non-linear transmission lines (NLTs), generating trains of short pulses with harmonic frequency content up to 400 GHz [8]. In contrast to an earlier version of the spectrometer [9] we now have integrated both NLTs in a single brass box, which is mounted directly on top of a cylindrical waveguide (lower cut-off at 80 GHz) of the sample holder in a dilution refrigerator. Infrared radiation is blocked by a black polyethylene window. This allows us to probe complex photoconductance in the 80–400 GHz range, corresponding to energies of 320  $\mu\text{eV}$ –1.6 meV. The typical charging energies of small dots are in the order of 0.5–1.5 meV, while the energies of the excited states in these dots are around 0.1–0.5 meV.

A top view is shown in Fig. 1(a): the NLTs are fed with two synthesizers (HP 83711A) connected on the left and right ports. The output of the two sources is then added by a power combiner and sent to a bow-tie antenna. The combiner and antenna circuit are defined by evaporating Au onto a Si substrate. The impedance of the whole circuit is matched to the 50  $\Omega$  antenna. The superimposed radiation of the NLTs is finally emitted into the cylindrical waveguide through a silicon hemisphere attached to the antenna on the back side of the circuit (see Fig. 1(b)) [10]. A close-up of one of the NLTs is given in Fig. 1(c). The meander shaped coplanar waveguide is intersected by voltage tunable Schottky diodes, leading to the pulse-forming response of the transmission line [11]. Although the output power of the sources is low to minimize heating, we observe a well-pronounced photoconductance signal.

Under wideband millimeter-wave radiation, the direct current through the dot is found to be increased (data not shown). In contrast to the appearance of single sidebands as found in photon-assisted tunneling on quantum dots, we observe a broad increase of the direct current, since about 50 harmonics of the 7.8 GHz base frequency are emitted simultaneously. Hence,

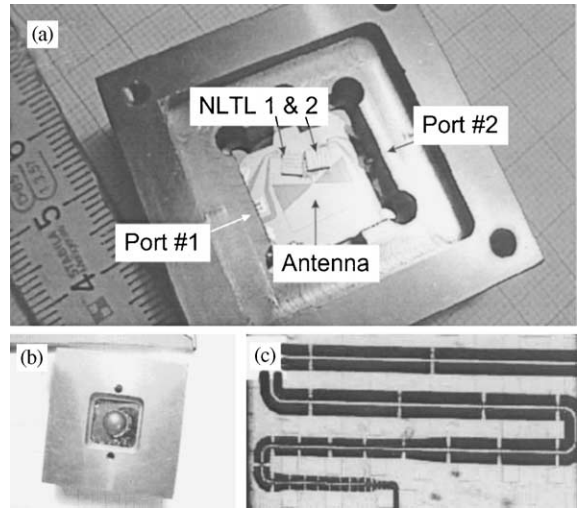


Fig. 1. (a) Top view of the heterodyne spectrometer circuit: the circuit is in the center of a brass box with two SMA ports feeding the two non-linear transmission lines (NLTs). The NLTs in turn feed a power combiner, which is terminated in the apex of the bow-tie antenna; (b) view of the silicon hemisphere on the bottom of the box, which optically couples the radiation into free space; (c) magnification of one of the meander-shaped transmission lines—the intersections are the position of the Schottky diodes.

a phase sensitive detection method is required to select the appropriate harmonic excitation, given a linear response. This is what the spectrometer provides: its two base frequencies of  $f_{1,2} = 7.8$  GHz are offset by  $\delta f = |f_2 - f_1| = 21$  Hz (see Fig. 2(a)). This allows selection of the corresponding harmonics with conventional lock-in techniques; the reference for the lock-in is taken from the beat note ( $\delta f$ ) of the two synthesizers. Phase locking the synthesizers enables a coherent detection of the photoconductance. With a two-channel lock-in amplifier we are able to monitor amplitude ( $A$ ), as well as the phase ( $\phi$ ) of the photoconductance at the corresponding excitation in the gigahertz range.

The quantum dot used in this particular experiment is realized in a GaAs/AlGaAs heterostructure by patterning the surface with conventional Schottky gates (split gates). The two-dimensional electron gas has an electron density of  $n_s = 1.7 \times 10^{15} \text{ m}^{-2}$  (not illuminated) and a mobility of  $40 \text{ m}^2 \text{ V}^{-1} \text{ s}^{-1}$ . The slopes of the diamond in Fig. 2(b) are  $\delta V_g / \delta V_{ds} = (C_R + C_g) / C_g = 3.42$  and  $\delta V_g / \delta V_{ds} = -C_L / C_g = -2.84$ ,

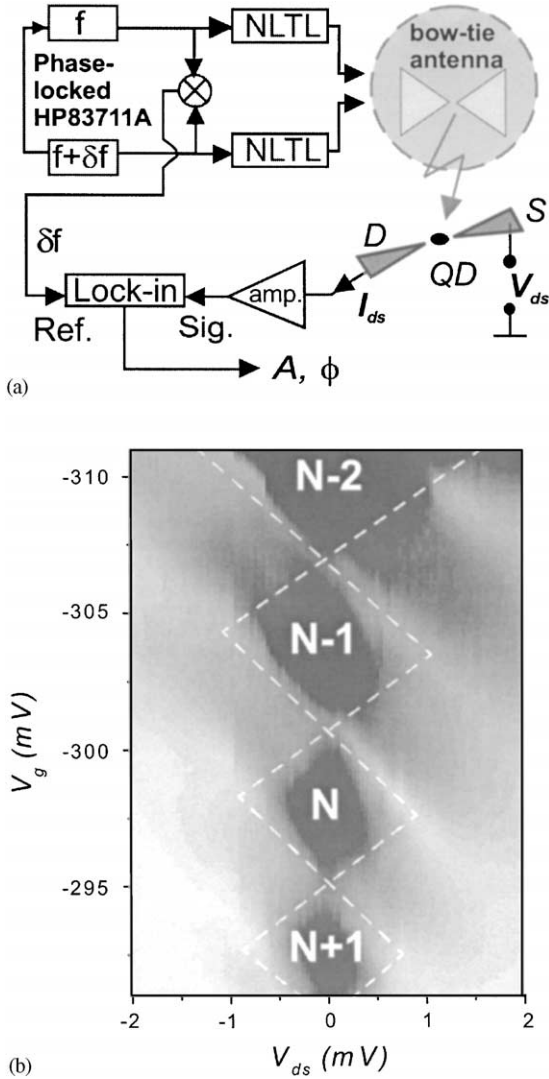


Fig. 2. (a) Schematic diagram of the setup: the two NLTLs are driven by synthesizers and the resulting radiation is fed through a waveguide onto the quantum dot sample and the photoconductance is measured; (b) grayscale plot of the conductance vs. drain/source relation of the quantum dot, measured with a conventional setup at a lock-in frequency of 137 Hz. From the diamond shapes we obtain the capacitances and the charging energy.

yielding a ratio  $\alpha = C_g / (C_L + C_R + C_g) = 0.16$ , where  $\alpha$  gives the scaling factor which relates the gate voltage ( $V_g$ ) to an energy scale. The capacitances of the dot to the left ( $C_L$ ) and right ( $C_R$ ) contact and to the gate ( $C_g$ ) are denoted, respectively. From the

diamond we obtain a charging energy of  $E_C = e^2/2C_\Sigma = 482 \mu\text{eV}$  ( $C_\Sigma$  being the total capacitance of the dot). The varying size of the diamonds indicates that the dot's total capacitance changes upon adding or removing a single electron—we estimate the 'electronic' dot radius to be 150 nm. The operating temperature of the  $^3\text{He}/^4\text{He}$  bath in the dilution refrigerator is  $T_b = 35 \text{ mK}$ , while the electron temperature in these measurements remains at  $T_e = 150 \text{ mK}$  under irradiation. In the grayscale plot of Fig. 2(b), hardly any fine structure indicating electron transmission through excited states is found.

In Fig. 3 two photoconductance spectra taken at the 12th harmonic of the spectrum (corresponding to 93.6 GHz (a)) and the 18th harmonic (corresponding to 140.4 GHz (b)) are given. The diamond shaped Coulomb blockade (CB) regions can be clearly identified, but in contrast to the grayscale plot of Fig. 2(b), which represents the conductance in the quasi-static limit, the measured amplitude in Fig. 3 represents the electron conductance induced by the millimeter-wave radiation. In this way it is possible to selectively determine the induced conductance at 93.6 and 140.4 GHz.

In general, we have to separate the response of the quantum dot into three different classes. Firstly, a bolometric response is found: a non-resonant pumping of electrons through the dot. Hence, we obtain in Fig. 3 CB diamonds similar to those in Fig. 2(b). Secondly, and most importantly, we observe fine structures in Fig. 3(a) and (b) in the single-electron tunneling regime. These are not present in the quasi-static conductance data of Fig. 2(b), and are related to microwave-induced resonant transitions through quantum dot states. These induced states are aligned parallel to the boundaries of the CB diamond, and hence are the ground states of the corresponding  $N$ -electron or  $(N + 1)$ -electron system. Comparing the excitation at 93.6 GHz  $\sim 388 \mu\text{eV}$  in Fig. 3(a) to the charging energy  $E_C$ , we find that the first microwave-induced transition opens a channel for the ground state of the  $(N + 1)$ -electron system (marked by the arrows at  $hf_\alpha = h93.6 \text{ GHz}$  in Fig. 3(a)). Varying the gate voltage further we find two additional resonant states  $N_1^*$ ,  $N_2^*$ , which can be attributed to excited states of the  $N$ -electron system. This scheme is repeated for the next diamond, although in this case only one excited state is detected ( $(N - 1)_1^*$ ). Changing the frequency leads to a shift of the ground state

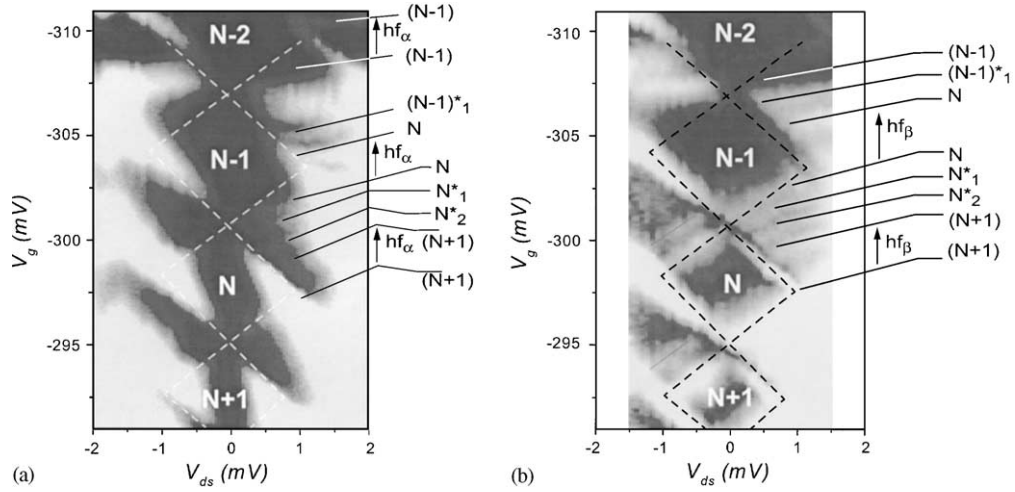


Fig. 3. (a) Grayscale representation of the high-frequency conductance  $G$  at the 12th harmonic,  $f = 12 \times 7.8 \text{ GHz} = 93.6 \text{ GHz}$  (black:  $G > 5 \mu\text{S}$ , white:  $G = 0 \mu\text{S}$ ). Drain/source bias is varied from  $-2$  to  $2 \text{ mV}$ . The diamond pattern represents the DC charging from Fig. 2 for comparison, while the excited states are indicated by the arrows on the right-hand side; (b) grayscale plot of the photoconductance at the 18th harmonic, an excitation frequency of  $f = 18 \times 7.8 \text{ GHz} = 140.4 \text{ GHz}$  (black:  $G > 5 \mu\text{S}$ , white:  $G = 0 \mu\text{S}$ ).

resonance as seen in Fig. 3(b), where a microwave energy of  $hf_\beta = h140.4 \text{ GHz} \cong 581 \mu\text{eV}$  lifts this state to exceed  $E_C$ . The excited states  $N_1^*$ ,  $N_2^*$  remain fixed in position relative to the ground states. It is important to note that this method allows microwave spectroscopy at finite bias. According to the capacitive coupling of the induced resonances, electrons absorb photons in the source contact. Variation of the gate voltage results in a shift of the discrete states in the quantum dot with respect to the source/drain bias. First the  $(N + 1)$ -ground state is excited, followed by the excited states of the  $N$ -electron system. The asymmetry of the tunneling barriers is revealed in the occurrence of excited states on only one side of the spectrum in Fig. 3.

The third effect of microwaves irradiating the dot is the shift of slopes of the diamond boundaries compared to the plot in Fig. 2(b). We find for the right-hand barrier a slope of only  $-0.54$ , and for the left-hand barrier  $2.58$  (upper-most diamond in Fig. 3(a)). Similar values are obtained for the signal at  $140.4 \text{ GHz}$ . Although for the following diamonds the values for both harmonics are closer to the ones in the quasi-static limit, we note that the capacitance of the left contact  $C_L$  shows a clearly different response in the photoconductance measurements. The

left-tunnel barrier is more transparent than the right one (see grayscale plot in Fig. 2(b)), hence we can assume that the radiation pumps the electrons out of (into) the dot through the right-tunnel barrier. Since these emptied (occupied) electronic states in the dot require a certain time to be reoccupied (emptied), the capacitance of the photoconductance measurements should be lower than the DC value. For the Coulomb diamonds below the first one, the tunnel coupling is obviously increased, leading to faster transfer rates of the electrons. The important time scale of this process is the repetition rate with which the pulsed microwave excitation induces transitions in the dot. Here this value is  $t_{\text{rep}} = 1/7.8 \text{ GHz} = 128 \text{ psec}$ , i.e. the radiation at  $93.6\text{--}140.4 \text{ GHz}$  excites electrons into energetically higher positions with an effective pumping rate of  $\sim 130 \text{ psec}$ . Hence, the pulse repetition rate allows the determination of the effective electron pumping rates. This also agrees with the effective time constant  $\tau \sim 1/RC$ : Assuming  $C = C_\Sigma \cong 166 \text{ aF}$  and a DC-resistance  $R \sim 1 \text{ M}\Omega$  of the tunnel barriers, we find a corresponding frequency of under  $6 \text{ GHz}$ , which is lower than the pulse repetition frequency.

In summary, we used a broadband millimeter-wave spectrometer for probing the dynamics of electrons confined in a quantum dot. This setup allowed us to

determine the high-frequency conductance in a fashion similar to the quasi-static limit. We found strong deviation of the dot's capacitances at millimeter-wave frequencies compared to the equilibrium values: a signature of the effective relaxation times of single-electron pumping. Moreover, we were able to monitor excited electron states in the quantum dot at finite bias.

We like to thank J.P. Kotthaus and K. von Klitzing for their continuous support and discussion. This work has been supported by the Deutsche Forschungsgemeinschaft, and the Bundesministerium für Wissenschaft und Technologie and DARPA (Ultrafast Electronics Program). One of us (H.Q.) acknowledges support by the Volkswagen foundation.

## References

[1] D. Loss, D.P. DiVincenzo, *Phys. Rev. A* 57 (1998) 120.

- [2] R. Ashoori, *Nature* 379 (1996) 413.
- [3] T.H. Oosterkamp, T. Fujisawa, W.G. van der Wiel, K. Ishibashi, R.V. Hijman, S. Tarucha, L.P. Kouwenhoven, *Nature* 395 (1998) 873.
- [4] H. Qin, A.W. Holleitner, K. Eberl, R.H. Blick, *Phys. Rev. B* 64 (2001) R241302.
- [5] T. Brandes, F. Renzoni, R.H. Blick, *Phys. Rev. B* 64 (2001) R035319.
- [6] Y. Nakamura, Y.A. Pashkin, J.S. Tsai, *Nature* 398 (1999) 786.
- [7] H. Qin, R.H. Blick, F. Simmel, A.W. Holleitner, J.P. Kotthaus, W. Wegscheider, M. Bichler, *Phys. Rev. B* 63 (2001) 35320.
- [8] D.W. van der Weide, F. Keilmann, U.S. Patent 5,748,309, May 5, 1998.
- [9] R.H. Blick, D.W. van der Weide, R.J. Haug, K. Eberl, *Phys. Rev. Lett.* 81 (1998) 689.
- [10] D.W. van der Weide, *Appl. Phys. Lett.* 62 (1993) 22.
- [11] D.W. van der Weide, *J. Opt. Soc. B* 11 (1994) 2553; D.W. van der Weide, *Appl. Phys. Lett.* 65 (1995) 881.